JOURNAL OF COMPUTATIONAL PHYSICS 77, 524–536 (1988)

# High-Order Newton–Cotes Integration Methods in Scattering Theory

BRYAN BASDEN AND ROBERT R. LUCCHESE

*Department of Chemistry, Texas A & M University, College Station, Texas, 77843*

Received May 22, 1987; revised October 27, 1987

We have implemented high-order Newton–Cotes integration formulas through 16th order for use in the integral equation formulation of scattering theory. We have found that the high-order integration rules give high accuracy results with fewer grid points than low-order rules. Use of Newton–Cotes formulas beyond 16th order was prohibited by numerical instabilities. These formulas were applied to both a model integral and to the calculation of the photoionization of $N_2$ leading to the $(2\sigma_u)^{-1}B^2\Sigma_u^+$ and $(3\sigma_g)^{-1}X^2\Sigma_g^+$ states of $N_2^+$ at a photon energy of 34 eV. High-order rules were found to be unstable when applied to the integration of functions which rise as $r^{2l+2}$ at high $l$ in the partial wave expansions. An empirical formula is presented which predicts when high-order rules diverge as a function of $l$ in a given integration region. Using a combination of high and low-order rules eliminated the divergence and still yielded accurate results in the $N_2$ photoionization calculations. Results for the photoionization of $N_2$ showed that Simpson's rule is the most efficient Newton–Cotes formula for calculations in which the desired error was larger than 0.14%. For smaller errors, high-order integration rules are more efficient. 

## I. INTRODUCTION

One of the computational bottlenecks to applications of non-relativistic quantum scattering theory to problems in molecular physics is that of finding a numerical integration technique which is both accurate and efficient for the evaluation of integrals of the form

$$I = \langle \alpha \,|\, V(GV)^n \,|\, \beta \rangle, \tag{1}$$

where $V$ is, in general, a non-local and non-spherically symmetrical interaction potential and $G$ is a non-local Green's function whose partial wave kernel is given by

$$g_l(r, r') = \begin{cases} s_l(r)\, c_l(r') & r < r' \\ c_l(r)\, s_l(r') & r > r' \end{cases}. \tag{2}$$

These integrals frequently occur in scattering theory, for example, in the use of variational functionals to compute scattering amplitudes [1–3], as well as in



0021-9991/88 $3.00

discretization methods for solving the Lippmann–Schwinger equation [4–10]. The choie of integration method is complicated by the fact that the operator $g_l(r, r')$ has a discontinuous derivative at $r = r'$. Methods of integration which do not adequately account for this discontinuity have poorly defined error estimates when such estimates depend on derivatives of the kernel [4].

Fraser [10] originated the idea of using Newton–Cotes quadrature formulas to overcome the difficulty associated with the discontinuity in the slope of the kernel of integral equations which occur in the theory of atomic and molecular scattering. Although Fraser discussed the possible use of higher order formulas, he only used the trapezoid rule [10]. The first use of higher order Newton–Cotes formulas in this class of integrals was the use of fourth-order formulas in the integration of the $1/r_{12}$ potential by Burgess *et al.* [11]. Note that the $1/r_{12}$ potential is the Green's function of the Laplacian and has a partial wave expansion of the form given in Eq. (2). Scattering equations have been solved using Newton–Cotes formulas of second order by Lucchese *et al.* [2] and of fourth order by Oza and Callaway [4]. Other approaches which adequately account for the discontinuity in the derivative include the use of integration formulas based on Chebyshev polynomials [6, 12], the Richardson extrapolation method [13], and the Rhomberg extrapolation method [3]. Methods based on the use of Gauss–Legendre quadratures, where the discontinuity is neglected, have also been used [9]. However, such methods have been shown [4, 5] to have convergence properties similar to those obtained using the trapezoid rule, which is the lowest order Newton–Cotes formula.

In many applications to systems of current interest, the evaluation of the integral over the Green's function takes significantly less time than computing the function over which the integrals are being taken. Thus, for a given level of accuracy, a more complicated integration procedure would be of great utility if it reduced the number of points at which the integrand must be evaluated. In large calculations of electron molecule scattering with several scattering channels, where much of the interchannel-coupling potential is long-range, and where angular effects arising from the nonspherical potential surface require that partial wave expansions be carried out to high $l$ [14], grid optimization is especially useful. Matrix multiplication between potential operators and scattering basis functions, which are defined at each grid point and each $l$, accounts for much of the computational effort in such calculations. Hence, savings in both computational effort and memory can be made by economic placement of grid points.

In this paper we derive the Newton–Cotes integration formulas of order 1, 2, 4, 8, and 16. We first apply these formulas to a simple model integral which illustrates the rapid convergence of the high-order rules. The high-order integration formulas are then applied to the fixed-nuclei two-state coupled-channel calculation of the photoionizaton of $N_2$ leading to the $(2\sigma_u)^{-1} B^2\Sigma_u^+$ and $(3\sigma_g)^{-1} X^2\Sigma_g^+$ states of $N_2^+$. In this system, difficulties were discovered in treating integrands of high partial waves which are of the form $r^{2l+2}$ for large $l$ and small $r$. A simple algorithm was generated for determining the best order integration to use in each integration region based on the fact that the high-order integration rules converge best if the

ratio, $r$(last)/$r$(first), where $r$(last) and $r$(first) are the upper and lower endpoints of the integration region, respectively, remains below a certain constant value. When this ratio becomes larger than a certain threshold, the trapezoid rule becomes the best rule to use, and the higher order rules diverge more rapidly. The 8th-order integration rule was found to give the best convergence for integrations which include the origin, for which the ratio described above is undefined. Using the apporpirate integration rule for each $l$ and integration region allowed us to avoid the divergence inherent in the high-order formulas. We found in the photoionization calculation on $N_2$ that Simpson's rule took fewer points when the maximum allowable error was greater than 0.14%. When the maximum allowable error was less than 0.14%, the high-order-rule grids were more efficient than Simpson's rule grids. The trapezoid rule was not found to be more useful than Simpson's rule under any acceptable level of accuracy. The error associated with high-order-rule grids was empirically found to be proportional to $(1/n)^{11.2}$, while that of Simpson's rule grids was proportional to $(1/n)^{2.8}$, where $n$ is the total number of points in the grid.

## II. Integration Formulas

The two-dimensional integrals which we will evaluate using the Newton–Cotes formulas may be represented by

$$I = \int v(\mathbf{r})\, G(\mathbf{r}, \mathbf{r}')\, v'(\mathbf{r}')\, d^3r\, d^3r'. \tag{3}$$

When $G(\mathbf{r}, \mathbf{r}')$ is the Green's function for a spherically symmetrical operator, the integral given in Eq. (3) can be written using a single center expansion of the form [2]

$$I = \sum_{l=0}^{\infty} \sum_{m=-l}^{l} \int_0^{\infty} dr'\, r'^2 v'_{lm}(r') \int_0^{\infty} dr\, r^2 v_{lm}(r)\, g_l(r, r'), \tag{4}$$

where $g_l(r, r')$ is the kernel of the Green's function of the form given in Eq. (2). In order to take into account the discontinuity in $g_l(r, r')$, we evaluate the inner integral,

$$f(r') = \int_0^{\infty} v_{lm}(r)\, g_l(r, r')\, r^2\, dr, \tag{5}$$

as a function of $r'$, splitting it along the discontinuity:

$$f(r') = c_l(r') \int_0^{r'} v_{lm}(r)\, s_l(r)\, r^2\, dr + s_l(r') \int_{r'}^{\infty} v_{lm}(r)\, c_l(r)\, r^2\, dr. \tag{6}$$

The first integral in Eq. (6) is referred to as the "forward integral," and the second integral the "backward integral" [4, 15].

The task of numerical integration is thus reduced to the evaluation of the forward and backward integrals of Eq. (6). We divide the overall integration space, 0 to $\infty$, into several integration regions, each of which contains a number of grid points consistent with the integration rule used. The step size between grid points is constant within each integration region, but each region may have a unique step size. The grid is truncated at some $r_{\max}$ which is chosen large enough so that the truncation error is of an acceptable size. The number of grid points needed to evaluate an integral using the $n$th-order Newton–Cotes formula is $n+1$. An integration rule may be used repetitively within an integration region, with common endpoints, so that the $n$th-order rule repeated $m$ times requires $nm+1$ points. We are able, then, to cover a region of 17 integration points with one 16th-order rule, two 8th-order rules, four 4th-order rules, or eight 2nd-order rules. Restricting ourselves to the use of these 4 integration rules allows for easy switching among rules. Examples of grids which use these integration rules in applications to the photoionization of $N_2$ are discussed in Section IV.

The Newton–Cotes integration weights are derived from Lagrange's interpolation formulas for equally spaced abscissa [16]. For each of the $n$th-order rules, a unique set of $n+1$ integration weights, $W_n[k, s]$, may be developed for evaluating the integral over each of the $n$ sub-regions, $x_0$ to $x_0+hs$, where $s$, the extent of the sub-region, ranges from 1 to $n$ and where $h$ is the step size between grid points. Integration weights for each sub-region are needed since $r'$, the point at which the integral in Eq. (6) is split, is not required to be at the boundaries of integration regions, but may be at any grid point, including those in the interior of an integration region. We may evaluate the integral, $I_s^n$, of some function $b$, from $x_0$ to $x_0+hs$ as

$$I_s^n = \int_{x_0}^{x_0+sh} b(x)\,dx = h\int_0^s b(x_0+ph)\,dp. \tag{7}$$

The value of the function, $b(x)$, at any point, $x=x_0+ph$, is approximately given by the Lagrange interpolation formula,

$$b(x_0+ph) \approx \sum_{k=0}^{n} A_k^n(p)\, b(x_0+kh), \tag{8}$$

where $A_k^n(p)$ is given by [16]

$$A_k^n(p) = \frac{(-1)^k}{k!(n-k)!(p-k+n/2)} \prod_{t=0}^{n} \left(p+\frac{n}{2}-t\right) \tag{9}$$

for even $n$, and

$$A_k^n(p) = \frac{(-1)^{k+1}}{k!(n-k)!(p-k+(n-1)/2)} \prod_{t=1}^{n+1} \left(p+\frac{n+1}{2}-t\right) \tag{10}$$

TABLE I

Weights at Each Point: 2nd-Order Rule

| Integration range | Points | | |
|---|---|---|---|
| | 0 | 1 | 2 |
| 0 to 1 | $\frac{5}{12}$ | $\frac{2}{3}$ | $-\frac{1}{12}$ |
| 0 to 2 | $\frac{1}{3}$ | $\frac{4}{3}$ | $\frac{1}{3}$ |

for odd $n$. Substituting the polynomial expression for $b(x_0+ph)$ given by Eq. (8) into Eq. (7) and integrating gives

$$I_s^n \approx h \sum_{k=0}^{n} b(x_0+kh)\, W_n[k, s], \tag{11}$$

where the Newton–Cotes weights, $W_n[k, s]$, are defined by

$$W_n[k, s] = \int_0^s A_k^n(p)\, dp. \tag{12}$$

Using MACSYMA [17], we were able to evaluate Eq. (12) analytically, and compute the integration weights as rational fractions. Tables I–III give these coefficients for integration rules of order 2, 4, and 8. Note that the weights in Table II for the rule of order 4 are identical to those given by Burgess *et al.* [11]. The weights in Table I are somewhat different from those given by Lucchese *et al.* [2]. The previously published second-order weights [2] have the advantage that they yield symmetric integrals (i.e., $\langle\alpha|\, VGV\,|\beta\rangle = \langle\beta|\, VGV\,|\alpha\rangle$) whereas the present formulas do not yield symmetric integrals. However, both second-order formulas give similar rates of convergence. The coefficients are available upon request for the 16th-order rule as well. Higher order rules are of little use since they have large integration weights (on the order of $10^4$ for the 32nd order) with oscillatory signs, giving rise to loss of accuracy on computers with fixed precision [18].

TABLE II

Weights at Each Point for the 4th-Order Rule

| Integration range | Points | | | | |
|---|---|---|---|---|---|
| | 0 | 1 | 2 | 3 | 4 |
| 0 to 1 | $\frac{251}{720}$ | $\frac{323}{360}$ | $-\frac{11}{30}$ | $\frac{53}{360}$ | $-\frac{19}{720}$ |
| 0 to 2 | $\frac{29}{90}$ | $\frac{62}{45}$ | $\frac{4}{15}$ | $\frac{2}{45}$ | $-\frac{1}{90}$ |
| 0 to 3 | $\frac{27}{80}$ | $\frac{51}{40}$ | $\frac{9}{10}$ | $\frac{21}{40}$ | $-\frac{3}{80}$ |
| 0 to 4 | $\frac{14}{45}$ | $\frac{64}{45}$ | $\frac{8}{15}$ | $\frac{64}{45}$ | $\frac{14}{45}$ |

TABLE III

Weights at Each Point for the 8th-Order Rule

| Integration range | Points 0 | 1 | 2 | 3 | 4 | 5 | 6 | 7 | 8 |
|---|---|---|---|---|---|---|---|---|---|
| 0 to 1 | $\frac{1070017}{3628800}$ | $\frac{2233547}{1814400}$ | $\frac{-2302297}{1814400}$ | $\frac{2797679}{1814400}$ | $\frac{-31457}{22680}$ | $\frac{1573169}{1814400}$ | $\frac{-645607}{1814400}$ | $\frac{156437}{1814400}$ | $\frac{-33953}{3628800}$ |
| 0 to 2 | $\frac{32377}{113400}$ | $\frac{22823}{14175}$ | $\frac{-21247}{56700}$ | $\frac{15011}{14175}$ | $\frac{-2903}{2835}$ | $\frac{9341}{14175}$ | $\frac{-15577}{56700}$ | $\frac{953}{14175}$ | $\frac{-119}{16200}$ |
| 0 to 3 | $\frac{12881}{44800}$ | $\frac{35451}{22400}$ | $\frac{1719}{22400}$ | $\frac{39967}{22400}$ | $\frac{-351}{280}$ | $\frac{17217}{22400}$ | $\frac{-7031}{22400}$ | $\frac{243}{3200}$ | $\frac{-369}{44800}$ |
| 0 to 4 | $\frac{4063}{14175}$ | $\frac{22576}{14175}$ | $\frac{244}{14175}$ | $\frac{32752}{14175}$ | $\frac{-1816}{2835}$ | $\frac{9232}{14175}$ | $\frac{-3965}{14175}$ | $\frac{976}{14175}$ | $\frac{-107}{14175}$ |
| 0 to 5 | $\frac{41705}{145152}$ | $\frac{115075}{72576}$ | $\frac{3775}{72576}$ | $\frac{159175}{72576}$ | $\frac{-125}{4536}$ | $\frac{85465}{72576}$ | $\frac{-24575}{72576}$ | $\frac{5725}{72576}$ | $\frac{-175}{20736}$ |
| 0 to 6 | $\frac{401}{1400}$ | $\frac{279}{175}$ | $\frac{9}{700}$ | $\frac{403}{175}$ | $\frac{-9}{35}$ | $\frac{333}{175}$ | $\frac{79}{700}$ | $\frac{9}{175}$ | $\frac{-9}{1400}$ |
| 0 to 7 | $\frac{149527}{518400}$ | $\frac{408317}{259200}$ | $\frac{24353}{259200}$ | $\frac{542969}{259200}$ | $\frac{343}{3240}$ | $\frac{368039}{259200}$ | $\frac{261023}{259200}$ | $\frac{111587}{259200}$ | $\frac{-8183}{518400}$ |
| 0 to 8 | $\frac{3956}{14175}$ | $\frac{23552}{14175}$ | $\frac{-3712}{14175}$ | $\frac{41984}{14175}$ | $\frac{-3632}{2835}$ | $\frac{41984}{14175}$ | $\frac{-3712}{14175}$ | $\frac{23552}{14175}$ | $\frac{3956}{14175}$ |

Odd orders of integration (e.g., 1, 3, 7, and 15) are used to compute the backward integral of Eq. (6) for the final integration region which contains the origin. We define our grids such that the first point is the first nonzero radial point [10]. The forward integrand is always zero at the origin and thus there is no need to compute the integrand there. The backward integrand is not always zero at the origin in applications to scattering theory, however, the value of the backward integral is never needed at the origin. Thus, if the same integration rules were used for both backward and forward integrations at the origin, we would have to extrapolate the integrand to determine its value at the origin even though we would not need to evaluate the backward integration past the first grid point. Use of the odd order of integration rules (one order less than the even order of integration used in the forward integration of the same region) avoids the need to extrapolate the integrand to the origin.

To illustrate the utility of high-order methods, we have applied integration rules of order 1, 2, 4, 8, and 16 to the integral given in Eq. (3) where we have used

$$v(\mathbf{r}) = v'(\mathbf{r}) = (4\pi)^{-1/2} e^{-|\mathbf{r}|} \tag{13}$$

and we have used the free particle Green's function which has an $l = 0$ kernel given by

$$g_{0,0}(r, r') = \begin{cases} (rr')^{-1} \sin(kr) \cos(kr') & r < r' \\ (rr')^{-1} \cos(kr) \sin(kr') & r > r'. \end{cases} \tag{14}$$

With these functions, the value of the integral given in Eq. (3) is then

$$I = -\frac{k(k^6 + 5k^4 + 15k^2 - 5)}{4(k^2 + 1)^4}. \tag{15}$$

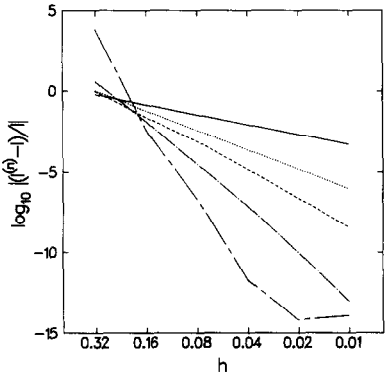


FIG. 1. Relative integration error as a function of step size for the integral defined by Eqs. (3), (13), and (14) for $k = 8.0$. The exact value of the integral is $I = -(567158/17850625)$. The different integration orders are: ———, the trapezoid rule; ···, Simpson's rule; – – –, the 4th-order rule; ——— · ———, the 8th-order rule; ——— — ———, the 16th-order rule.

In Fig. 1 we give the relative error in the integral as a function of the step size $h$ for the five integration rules considered here for $k = 8$ and where the radial integrals were terminated at $r_{max} = 40.96$. Three features of the data presented in Fig. 1 illustrate the advantages and limitations of the high-order Newton–Cotes integration formulas. The first feature is that the high-order methods converge more rapidly than low-order methods as $h$ decreases. The second feature is that as $h$ is increased the high-order integration methods diverge more rapidly than the low-order rules. Thus when applying high-order integration methods, one must be careful to choose the step sizes small enough so that the integrals are convergent. This point will be discussed in detail in Section III when we consider the integration of rapidly varying integrands. The third feature which is evident in Fig. 1 is that the maximum accuracy of the 16th-order integration is 1 part in $10^{14}$. These calculations were performed using double precision arithmetic on DEC VAX 11/780 for which the real numbers a represented with a precision of 1 part in $10^{16}$. This loss of accuracy is due to the fact that the coefficients of the order 16 integration formulas have a maximum magnitude of $\sim 200$ and have alternating signs. As mentioned above, integration rules of order greater than 16 have further restricted accuracies due to large and oscillatory integration weights.

## III. Divergence with Integrands of the Form $r^{2l+2}$

Although high-order Newton–Cotes integration schemes converge very quickly when applied to functions which vary slowly, some difficulty was encountered in applying these schemes to the Green's function for high partial waves, where both the regular Green's function, $s_l(r)$, and the wave function, $v_{lm}$, rise as $r^l$ near the origin, resulting in an integrand with an $r$ dependence of the form, $r^{2l+2}$. At high $l$'s,

the high-order integration rules diverge because of the rapid rise in the function. For example, consider the use of the 16th-order rule to integrate over the subregion between the 0th and 1st grid points of a 17-point region in which the integral is rising rapidly. While the last few grid points of this 17-point region have very small integration weights and should contribute very little to the value of the integral up to the 1st point, these final grid points add a divergently large quantity to the value of the integral. As discussed below, this difficulty can be overcome by selecting different integration rules for the same grid points based on the partial wave being integrated.

An algorithm for choosing the rule which converges best in a given grid region was developed by studying the convergence of each integration rule as a function of $\lambda$, the total exponent of $r$ in the forward integrand (i.e., $\lambda = 2l + 2$). We conducted studies on the quadrature error in the evaluation of the integral

$$f_{i+1}(a+hs) = \frac{\lambda+1}{(a+hs)^{\lambda+1} - a^{\lambda+1}} \int_a^{a+hs} f_i(x')(x')^{\lambda}\, dx', \tag{16}$$

where we have taken

$$f_1(x) = 1. \tag{17}$$

We have defined $f_{i+1}(a+hs)$ so that it will only differ from $f_i(a+hs)$ as a result of integration error, and we determine the integration error, $E(n)$, by comparing $f_1(a+hs)$ with successive values of $f_i(a+hs)$ which are computed iteratively using the quadrature approximation

$$f_{i+1}(a+hs) = \frac{h(\lambda+1)}{(a+hs)^{\lambda+1} - a^{\lambda+1}} \sum_{k=0}^{n} W_n[k, s] f_i(a+hk)(a+hk)^{\lambda}, \qquad s = 1, \ldots, n, \tag{18}$$

where $h$ is the step size. We have computed $f_i(a+hs)$ up to $i = 11$ since functions of the form $f_{11}(x)$ occur in some of the matrix elements of the Padé approximant method used in Section IV. Thus, we defined $E(n)$ according to

$$E(n) = \max |f_i(a+hs) - 1|_{s=1,\ldots,n}^{i=1,\ldots,11}. \tag{19}$$

At each order of integration, we compute $E(n)$ for $\lambda = 20$, 30, 40, and 50, and for the ratios,

$$R = \frac{a+hn}{a}, \tag{20}$$

at $R = 1.25$, 1.5, 2.0, 3.0, and 5.0. In comparing the different integration rules in Fig. 2, the step size was held constant for all integration orders, so that a ratio of 5.0 for the 16th-order rule is compared to a ratio of 3.0 for the 8th-order rule, etc.

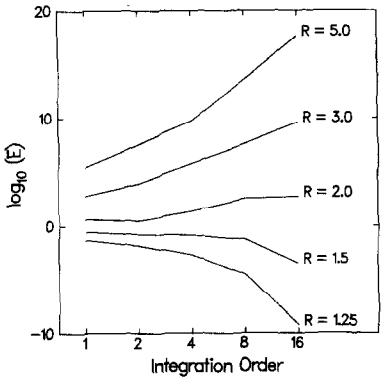


FIG. 2. Integration error, defined in Eq. (19) for $\lambda = 30$, as a function of the order of integration for various ratios, $R$, defined in Eq. (20) for the 16th-order rule.

Figure 2 shows the results for $\lambda = 30$. For $R = 1.25$ and 1.5, $E(16) < E(1)$, while for the other ratios, the order is inverted. There is, therefore, a value of $R$ at which the convergence switches from preferring the 16th-order rule to the trapezoid rule for each value of $\lambda$. The value of $R$ at the switch point, $R_s(\lambda)$, was determined by plotting $\log[E(16)] - \log[E(1)]$ versus $R$, and taking the value of $R$ for which

$$\log(E(16)) - \log(E(1)) = 0. \tag{21}$$

It was discovered that the plot of $n$ defined as

$$n = \frac{\log[R_s(x) - 1]}{\log(2)} \tag{22}$$

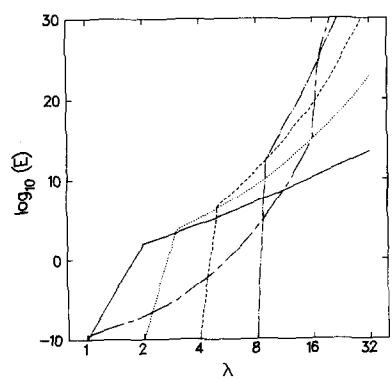


FIG.3. Integration error defined by Eq. (19) as a function of $\lambda$ for a region beginning with the origin: ———, the trapezoid rule; ···, Simpson's rule; – – –, the 4th-order rule; ——— · ———, the 8th-order rule; ——— – – ———, the 16th-order rule.

versus $1/\lambda$ gives a straight line with a slope of 86.6 and an intercept of $-3.30$. This information allows us to determine whether the 16th-order rule or the trapezoid rule is best for a given $R$ and $\lambda$. While this eliminates the problem of divergent integrals, it does limit the use of the high-order integration formulas.

A similar analysis was done for the special case of an integration region which begins with the origin, for which the ratio $R$ is undefined. Figure 3 shows the errors found for the various integration orders as a function of $\lambda$. The data illustrates the numerical instability in the 16th-order rule for regions which begin at the origin. We conclude that the optimal integration formula for use at the origin is the 8th-order rule through $\lambda = 8$, which corresponds to $l = 3$, and then for higher $l$'s, the trapezoid rule is less divergent.

## IV. Applications to the Photoionization of $N_2$

The fixed-nuclei two-state coupled-channel calculation of the photoinization leading to the $(2\sigma_u)^{-1} B^2\Sigma_u^+$ and $(3\sigma_g)^{-1} X^2\Sigma_g^+$ states of $N_2$ was chosen to test the high-order Newton–Cotes methods since it is a case of current theoretical interest [1], and since the development of more optimized grids was a computational prerequisite for future work in this area. Tests were done on the $2\sigma_u \to k\sigma_g$ and $3\sigma_g \to k\sigma_u$ contributions to the photoionization at a photon energy of 34 eV since effects of the channel coupling make the cross sections and asymmetry parameters at this energy very sensitive to small changes in the grid. The scattering equations were solved via the multichannel $\tilde{C}$-functional approach with Padé-approximant corrections [1–2, 19–22], where the variational functional was

$$\mathbf{M}^3_{35}(\boldsymbol{\phi}_t, \mathbf{r}, \boldsymbol{\phi}^c_E) = \langle \boldsymbol{\phi} | \, \mathbf{r} \, | \boldsymbol{\phi}^c_E \rangle + \langle \boldsymbol{\phi}_t | \, \mathbf{r}\mathbf{G}_c\mathbf{V}_Q \, | \boldsymbol{\phi}^c_E \rangle + \langle \boldsymbol{\phi}_t | \, \mathbf{r}\mathbf{G}_c\mathbf{V}_Q\mathbf{G}_c\mathbf{V}_Q \, | \boldsymbol{\phi}^c_E \rangle$$
$$+ \sum_{\alpha,\beta} \langle \boldsymbol{\phi}_t | \, \mathbf{r}\mathbf{G}_c\mathbf{V}_Q\mathbf{G}_c\mathbf{V}_Q | \boldsymbol{\alpha} \rangle \langle \mathbf{V}_Q - \mathbf{V}_Q\mathbf{G}_c\mathbf{V}_Q \rangle^{-1}_{\alpha\beta} \langle \boldsymbol{\beta} | \, \mathbf{V}_Q\mathbf{G}_c\mathbf{V}_Q \, | \boldsymbol{\phi}^c_E \rangle, \tag{23}$$

where $\mathbf{V}_Q$ is the Phillips–Kleinman pseudopotential [2, 23], $\mathbf{r}$ is the dipole operator, $\mathbf{G}_c$ is the matrix of channel Coulomb Green's functions [1], and $\boldsymbol{\phi}^c_E$ are the vectors of channel Coulomb waves [1, 20]. The $r_{\max}$ was taken to be 163.8 a.u.

The grid on which the calculations were performed was chosen by a local optimization method. The first step in the optimization was to divide the radial integration into several regions based on the rate of change of the occupied orbitals and their derivatives. Note that the target wave function of $N_2$ was constructed from linear combinations of Gaussian functions centered at the nuclei. Thus at the radius which corresponds to the position of the nuclei the orbitals are very rapidly changing, which in turn means that the grid step size must be small near the nuclei. In each region the step size is chosen to converge a test integral of the type used in the actual calculation to within a specified tolerance. We computed three different types of grids. The first grid was composed of all first-order, i.e., trapezoid, rules and the second was composed of all second-order, i.e., Simpson's, rules. For the

third type of grid, the optimizatin procedure also considered different rules for a particular region and chose the most efficient rule in addition to the appropriate step size. This optimization procedure did not necessarily produce the globally optimum grid but could only give a grid which was locally optimum in each integration region considered. The most accurate grid containing high-order integration rules obtained from the optimization procedure is given in Table IV. To obtain a standard result by which the accuracy of all of the optimized grids were judged, the density of points of the high accuracy grid given in Table IV was doubled to yield a grid of 2120 points. For each grid the photoionization of $N_2$ was calculated yielding 8 cross sections, 4 from each channel, the length and velocity forms [14] of the asymmetry parameter and the length and velocity forms of the cross section. An overall error for each calculation was computed as the root-mean-square of the deviations of these 8 results in comparison with the corresponding standard result obtained from the grid with 2120 points. A log–log plot of the RMS deviation as a function of the number of grid points was found to be approximately linear as shown in Fig. 4.

The slope of the line for the high-order grids was found to be $-11.2 \pm 0.6$, while the Simpson's rule slope was found to be $-2.7 \pm 0.3$, and the trapezoid rule slope was $-1.7 \pm 1.0$. This demonstrates that even in a full calculation with the difficulties mentioned above, the high-order rules converge much faster than low-order rules. The high-order grids and the Simpson's rule grids cross at an RMS deviation of 0.0014. Calculations in which the required accuracy is less than this may be accomplished more efficiently with use of the Simpson's type grid. The flexibility of the Simpson's rule is thought to enable it to perform better than the high-order rules at low accuracies. Step sizes may be changed more often in a rule which is defined by only 3 points, so that the step size remains optimal. In the high-order-rule grids,

TABLE IV

Optimized High-Order Grid Containing 1060 Points[a]

| Region | Points | Order | Step size | End (a.u.) |
|---|---|---|---|---|
| 1 | 88 | 8 | 0.0106 | 0.929 |
| 2 | 16 | 8 | 0.0043 | 0.998 |
| 3 | 24 | 4 | 0.0015 | 1.034 |
| 4 | 20 | 4 | 0.0018 | 1.070 |
| 5 | 16 | 16 | 0.0057 | 1.161 |
| 6 | 16 | 16 | 0.0160 | 1.417 |
| 7 | 16 | 16 | 0.0359 | 1.991 |
| 8 | 16 | 16 | 0.0567 | 2.898 |
| 9 | 16 | 16 | 0.0822 | 4.214 |
| 10 | 32 | 16 | 0.0987 | 7.370 |
| 11 | 16 | 16 | 0.1184 | 9.265 |
| 12 | 624 | 16 | 0.1994 | 133.691 |
| 13 | 160 | 16 | 0.1882 | 163.800 |

[a] Note that the nucleus in $N_2$ is at $r = 1.034$ a.u.

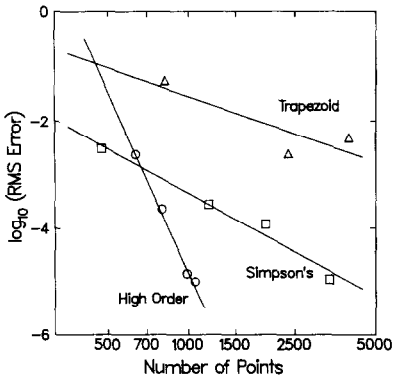


FIG. 4. Root-mean-square deviation in the asymmetry parameters and cross sections of the $2\sigma_u \rightarrow k\sigma_g$ and $3\sigma_g \rightarrow k\sigma_u$ contributions to the photoionization of $N_2$ as a function of the number of grid points for the high-order rules, Simpson's rule, and the trapezoid rule, at a photon energy of 34 eV.

points are added inefficiently to the grids simply because they are needed to define the integration.

The trapezoid rule was found to be inferior to both the Simpson's rule and higher order rules. This conclusion is consistent with that of previous studies [4–5] in reiterating that the trapezoid rule, and by extension the Gauss-Legendre quadratures, are not efficient in comparison with higher order Newton–Cotes integration formulas.

## V. CONCLUSIONS

We have shown that at low accuracies Simpson's rule is efficient in providing integrals of Green's functions which have kernels with discontinuous first derivatives. We have also shown that the high-order Newton–Cotes formulas may be implemented to provide rapid convergence to a high degree of accuracy. The availability of accurate integration methods will have at least two important applications in studies of electron-molecule scattering such as the study of the photoioniation of $N_2$. First, in variational methods [1–3], basis sets which are nearly linearly dependent lead to numerically unstable results with low accuracy integration methods, but should give stable results with high accuramcy methods. And second, the availability of accurate results allows one to determine absolute errors in less accurate but smaller grids which can then be used to efficiently compute the needed cross sections at an acceptable level of accuracy.

## ACKNOWLEDGMENTS

Acknowledgment is made to the Monsanto Company, the Dow Chemical Company Foundation, and the Celanese Chemical Company for partial support of this research. In addition, this material is based upon work supported in part by the National Science Foundation under Grant CHE-8351414 and in part by the Robert A. Welch Foundation under Grant A-1020.

## REFERENCES


1. B. BASDEN AND R. R. LUCCHESE, *Phys. Rev. A* **34**, 5158 (1986).
2. R. R. LUCCHESE, K. TAKATSUKA, AND V. MCKOY, *Phys. Rep.* **131**, 149 (1986).
3. J. HORACEK AND T. SASAKAWA, *Phys. Rev. C* **32**, 70 (1985).
4. D. H. OZA AND J. CALLAWAY, *J. Comput. Phys.* **68**, 89 (1987).
5. M. S. STERN, *J. Comput. Phys.* **25**, 56 (1977).
6. M. S. STERN, *J. Comput. Phys.* **28**, 122 (1978).
7. P. S. DARDI, S. SHI, AND W. H. MILLER, *J. Chem. Phys.* **83**, 575 (1985).
8. L. M. HUBBARD, S. SHI, AND W. H. MILLER, *J. Chem. Phys.* **78**, 2381 (1983).
9. B. I. SCHNEIDER AND L. A. COLLINS, *Phys. Rev. A* **33**, 2970 (1986).
10. P. A. FRASER, *Proc. Phys. Soc.* **78**, 329 (1961).
11. A. BURGESS, D. G. HUMMER, AND J. A. TULLY, *Philos. Trans. Roy. Soc. London* **226**, 225 (1970).
12. S. E. EL-GENDI, *Comput. J.* **12**, 282 (1969).
13. G. PAIANO AND S. L. PAVERI-FONTANA, *J. Phys. A* **13**, 3287 (1980).
14. R. R. LUCCHESE, G. RASEEV, AND V. MCKOY, *Phys. Rev. A* **25**, 2572 (1982).
15. R. R. LUCCHESE AND V. MCKOY, *Phys. Rev. A* **21**, 112 (1980).
16. P. J. DAVIS AND I. POLONSKY, in *Handbook of Mathematical Functions*, Appl. Math. Series Vol. 55, edited by M. Abramowitz and I. A. Stegun (National Bureau of Standards, Washington D.C., 1972), p. 875.
17. Symbolics, computer code *MACSYMA* (Symbolics Inc., Cambridge, MA, 1985).
18. K. E., ATKINSON, *An Introduction to Numerical Analysis* (Wiley, New York, 1978), p. 225.
19. R. R. LUCCHESE AND V. MCKOY, *Phys. Rev. A* **28**, 1382 (1983).
20. R. R. LUCCHESE, *Phys. Rev. A* **33**, 1626 (1986).
21. M. T. LEE, K. TAKATSUKA, AND V. MCKOY, *J. Phys. B* **14**, 4115 (1981).
22. K. TAKATSUKA AND V. MCKOY, *Phys. Rev. A* **23**, 2352 (1981).
23. J. D. WEEKS, A. HAZI, AND S. A. RICE, in *Advances in Chemical Physics*, Vol. XVI, edited by I. Prigogine and S. A. Rice (Interscience, New York, 1969), p. 283.